Removal of methylene blue from aqueous solutions using an Fe^{2+} catalyst and *in-situ* H_2O_2 generated at gas diffusion cathodes

Engracia Lacasa[1], Pablo Cañizares[2], Frank C. Walsh[3], Manuel A. Rodrigo[2], Carlos Ponce-de-León[3]*

[1] Department of Chemical Engineering, School of Industrial Engineering, University of Castilla-La Mancha, 02071 Albacete, Spain

[2] Department of Chemical Engineering, Faculty of Chemical Sciences and Technologies, University of Castilla-La Mancha, 13005 Ciudad Real, Spain

[3] Electrochemical Engineering Laboratory, Energy Technology Research Group, Faculty of Engineering and Physical Sciences, University of Southampton, SO17 1BJ, Highfield Southampton, United Kingdom

Abstract

Textile industries generate large volumes of wastewater containing organic dyes, which may be hazardous to the environment and human health. In this work, the oxidation of 100 mg dm^{-3} of methylene blue (MB) in aqueous solutions was studied using H_2O_2 (formed *in-situ*) at gas diffusion electrodes (GDEs) in the presence of 1×10^{-3} mol dm^{-3} Fe^{2+} catalyst, to create hydroxyl radicals to facilitate Fenton oxidation. The influence of applied potential (-0.5 to -1.3 V *vs*. Ag/AgCl) at different oxygen flow rates to the GDE (0.15 – 0.45 cm^3 min^{-1}) and different counter electrode materials (Pt mesh, Ni mesh, RVC) was investigated. MB was completely degraded to a residual concentration below the detection limit of 0.5 mg dm^{-3}. The rate and degree of mineralisation were significantly influenced by the applied potential. A maximum mineralisation of 88.2%

was achieved at -1.0 V *vs.* Ag/AgCl. The oxygen flow rate to the GDE did not influence the degradation of MB under the experimental conditions. The counter electrode material affected the degree of mineralisation in the order Pt mesh > reticulated vitreous carbon (RVC) > Ni mesh. The apparent first order rate decay constant for MB degradation and MB mineralisation was calculated to have a maximum value of 0.0182 min^{-1} for MB mineralisation at a potential of -1.0 V *vs.* Ag/AgCl.

Keywords: electrochemical oxidation, electro-Fenton process, gas diffusion electrode, methylene blue.

* Corresponding author.

E-mail address: C. Ponce-de-León: capla@soton.ac.uk

E. Lacasa: engracia.lacasa@uclm.es

1. Introduction

The presence of organic dyes in aqueous effluents is a major concern due to their environmental persistence and adverse effects on human health. Even at low concentrations (less than 1 ppm), dyes are highly visible and may interfere with photosynthesis by consuming oxygen needed for living species. The textile industry consumes large volumes of water in the colour process products; a considerable amount of coloured wastewater is generated, which contributes over 20% of the total water pollution [1, 2]. Among these dyes, methylene blue, MB is one of the most common colorants in the textile industry for dyeing cotton, wood and silk. The ingestion of water containing MB can cause nausea, vomiting, profuse sweating, mental confusion and methemoglobinemia [3-5]. According to the commission regulation (EU) 2015/830, the safety data sheet shows that LD50 was fixed up to 1.18 g kg^{-1} in rats for MB ingestion. Therefore, the treatment of aqueous effluents containing MB is important due to its hazardous impact on receiving waters.

The removal of dyes from aqueous solutions have been widely studied by physicochemical [6-11], chemical [12, 13], microbiological [14], electrochemical [15-17] and advanced oxidation processes (AOPs) [18-21]. Electrochemical approaches have been developed for use in aqueous effluent treatment and show improved environmental compatibility, high energy efficiency, automation and safety [19, 22, 23].

The electro-Fenton process has been used for the environmental prevention of organic dye pollution in aqueous effluents for over 3 decades. This approach offers significant

advantages compared to the traditional Fenton's reagent method such as: facile regulation of *in-situ* H_2O_2 production, higher degradation rates of the organic pollutants due to the faster regeneration of the Fe^{2+} catalyst at the cathode and lower operating costs when experimental variables are optimised [19, 24].

The electro-Fenton process is an indirect anodic oxidation based on the production of hydroxyl radicals (•OH) from the Fenton process in reaction (1), between catalytic Fe^{2+} ion present in the bulk of the solution and H_2O_2 generated at a suitable cathode, using an optimum pH near to 3.0. Hydroxyl radicals are well known to have one of the highest oxidising potentials (E^0 = 2.80 V *vs.* SHE) and are extremely reactive with most organic pollutants, showing relatively high rate constants in the range from 10^7 to 10^{10} dm^3 mol^{-1} s^{-1} [25].

$$Fe^{2+} + H_2O_2 \rightarrow Fe^{3+} + \bullet OH + OH^- \quad (1)$$

Ferrous ions are continuously regenerated from Fe^{3+} reduction at the cathode according to reaction (2), avoiding the production of sludge and promoting a higher rate of degradation.

$$Fe^{3+} + e^- \rightarrow Fe^{2+} \qquad E^0 = 0.77 \text{ V } vs. \text{ SHE} \quad (2)$$

H_2O_2 is continuously produced by the two-electron cathodic reduction of dissolved oxygen, according to reaction (3).

$$O_2 + 2H^+ + 2e^- \rightarrow H_2O_2 \qquad E^0 = 0.68 \text{ V } vs. \text{ SHE} \quad (3)$$

Oxygen gas may be supplied to the cathode by bubbling oxygen into the bulk of the solution or by feeding oxygen or air through a GDE. The latter electrodes are preferred

since they increase the process efficiency significantly compared to bubbling O_2 through the solution, as they are not limited by the low oxygen solubility [26-28]. The manufacture of gas diffusion electrodes is already an established technology in fuel cells and chlorine production and their use for hydrogen peroxide generation needs more studies to characterise the flow of oxygen towards the catalyst layer and to remove the water to avoid flooding of the electrode on the gas side. In addition GDE help to decrease the energy utilisation during the degradation of organic materials.

The most suitable cathodes for reaction (3) include carbonaceous materials with high surface area, such as carbon nanotubes [29, 30], graphite felt [31, 32], activated carbon fibre [33], carbon modified with metals or metal oxide nanoparticles [34], carbon felt [35, 36], carbon-polytetrafluoroethylene (PTFE) composites [37, 38], reticulated vitreous carbon (RVC) [39, 40] and boron doped diamond (BDD) [41].

The aim of this paper is to evaluate the removal of MB (selected as a model organic dye) in aqueous solutions by using hydroxyl radicals formed from H_2O_2 generated *in-situ* at a GDE catalysed by Fe^{2+} ions. The influence of the applied electrode potential (-0.5 to -1.3 V *vs.* Ag/AgCl), the oxygen flow rate (0.15 – 0.45 cm^3 min^{-1}) and the counter electrode material (Pt mesh, Ni mesh and RVC) was studied in order to determine their effect on the mineralisation rate of methylene blue in an electrochemical cell operating in the batch mode. To the authors' knowledge, the influence of the counter electrode material on the electro-Fenton process by using gas diffusion cathodes has not previously been reported in the literature.

2. Materials and methods

2.1. Chemicals

Methylene blue, sodium sulphate and iron chloride were of analytical grade (> 98% purity) purchased from Fisher Scientific. Other chemicals employed such as nitric, hydrochloric and sulfuric acids and potassium permanganate were also analytical grade from the same source. All solutions were prepared with ultra-pure water obtained from a SUEZ Water UK system, with a resistivity > 18.2 MΩ cm at 23 ºC.

2.2. Construction of the gas diffusion electrode

The gas diffusion electrode (GDE) was constructed by a similar method to that previously reported in literature [42, 43]. The GDE structure involved a gas diffusion layer on top of a carbon cloth and a nickel current collector, bound together in a single hot-pressing step. The size of the gas diffusion layer was 50 × 20 mm on 0.11 mm thickness carbon cloth previously treated on one side with 25 wt. % PTFE (FuelCell.com). A homogeneous paste, consisting of 80 wt.% carbon black powder (Vulcan® XC72R carbon black, from Cabot), 20 wt.% of PTFE (60 *wt*.% dispersion in H_2O from Sigma Aldrich) and 10 cm^3 of water per 1 g of solids, was rolled over the carbon cloth using the doctor blade technique. The current collector was a piece of expanded nickel mesh (Dexmet, 32 mesh, 0.05 mm thick) which was placed on the top of the gas diffusion layer. Finally, the GDE was placed in a hydraulic press (Carver, model 3851) and pressed for 10 minutes at a temperature of 0 °C under 15 kN m^{-2} pressure, followed by 10 min in an oven at 340 ºC then left to cool down to room temperature (25 ºC) at atmospheric pressure.

2.3. Experimental procedures

The electrochemical experiments were carried out in an undivided, 3-electrode glass cell shown in Fig. 1. Platinum, nickel mesh or reticulated vitreous carbon (RVC) were used as counter electrodes, Ag/AgCl (sat'd KCl) was used as reference electrode with a GDE working electrode, which was replaced for each experiment. The reference electrode was inserted into a Luggin capillary, approx. 2 mm from the working electrode. The area of the GDE exposed to the solution was 1 cm^2, although the active surface area of the GDE was expected to be much larger because of the high porosity of carbon black/PTFE mixture, that enhances the mass transport of oxygen within the porous structure [44]. The temperature was maintained at 25 ºC using a thermostatic bath (Julabo). Oxygen flowed to the rear, hydrophobic side of the GDE at rates between 0.15 and 0.45 $cm^3\ min^{-1}$, with the gas exit open to the atmosphere. A potentiostat/galvanostat instrument (Ivium-n-Stat, Ivium Technologies) was used to control the electrode potential.

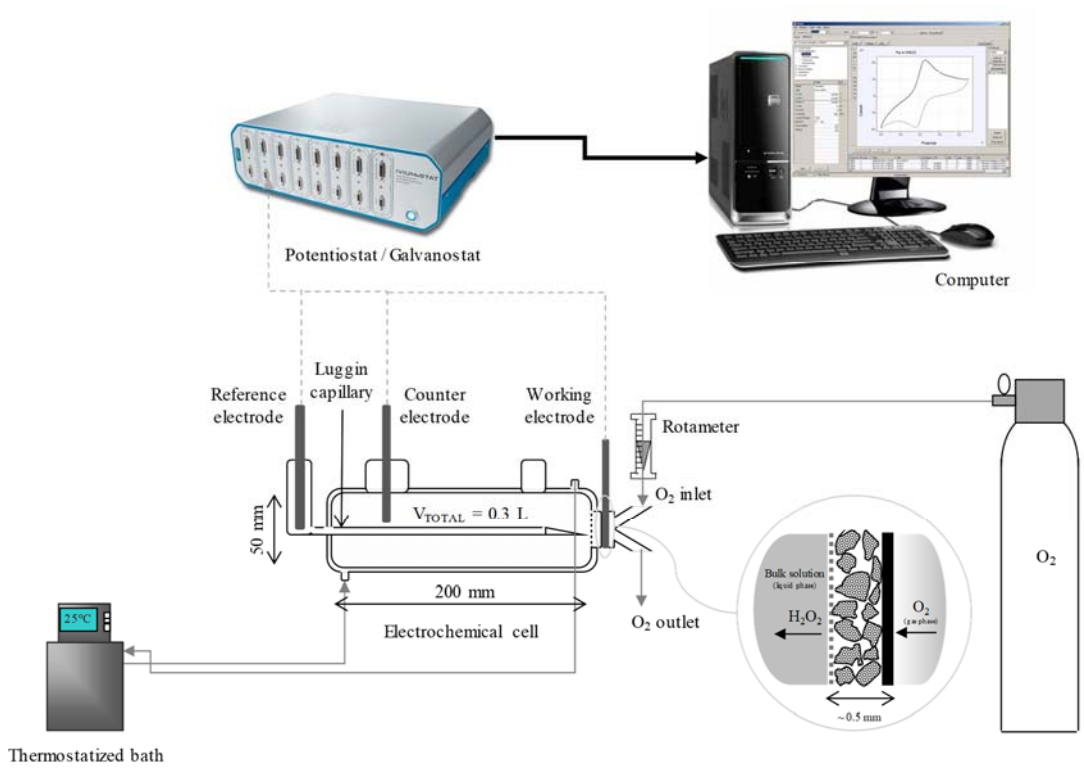

Fig. 1. Experimental arrangement of the electrolysis cell, which incorporated a GDE.

Synthetic wastewater was prepared with 100 mg dm^{-3} of MB as pollutant, 50×10^{-3} mol dm^{-3} of Na_2SO_4 as supporting electrolyte and 1×10^{-3} mol dm^{-3} of Fe^{2+} ($FeCl_2 \cdot 4H_2O$) as catalyst to initiate the electro-Fenton process [26]. The initial pH of the solution was adjusted to pH ≈ 3 with sulfuric acid and measured with pH test strips at the start of each experiment. All experiments were carried out under potentiostatic conditions at potentials applied between -0.5 and -1.3 V *vs.* Ag/AgCl. The synthetic wastewater was added to the glass cell and agitated vigorously by a magnetic, PTFE coated steel stirrer (1000 rpm), centrally located at the bottom of the cell in order to enhance the mass transport; samples of 5 cm^3 were collected at regular intervals of time to analyse the MB decolourisation, H_2O_2 concentration and total organic carbon (TOC).

2.4 Analytical procedures

The degradation of MB was determined by an UV-Vis spectrophotometer (Scinco Neosys 2000). Stock solutions of MB were prepared from 0.1 to 100 mg dm^{-3} in order to obtain their absorbance scans in a wavelength range between 200 and 800 nm. Here, the maximum absorbance for MB was determined at a wavelength of 664 nm. MB concentrations and their respective absorbance at 664 nm were plotted to obtain the linear calibration curve. Eq. (4) with a correlation factor of 0.9942, was used to calculate the MB decolourisation (c_{MB}).

$$c_{MB} \text{ /mg dm}^{-3} = 6.5783\, A_{\lambda = 664\text{ nm}} \quad (4)$$

Where c_{MB} and A are the concentration and the absorbance of methylene blue. Hydrogen peroxide concentration was determined with permanganate according to a standard method [45]. A mixture 4:1 (v/v) of sample: H_2SO_4 was titrated with 4×10^{-3} mol dm^{-3}

$KMnO_4$ until a faint pink colour was achieved. The Total Organic Carbon (TOC) was determined using a Shimadzu TOC-V_{CPH} analyser.

3. Results and discussion

Fig. 2 shows the influence of the applied electrode potential on the MB dye degradation during the electrolysis of synthetic wastewater containing 100 mg dm^{-3} of MB and 1 × 10^{-3} mol dm^{-3} of $FeCl_2$. The curves show the degradation of MB at four electrode potentials within the range of the highest production of hydrogen peroxide, i.e. from -0.5 V to -1.3 V *vs.* Ag/AgCl.

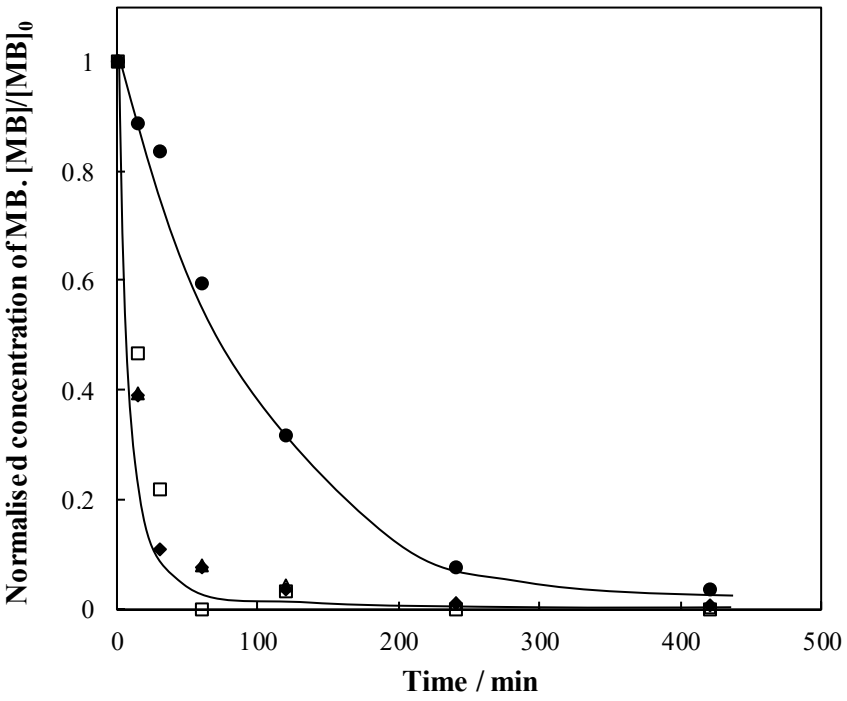

Fig. 2. The influence of applied potential electrode on the degradation of MB during the electrolysis. Working electrode: carbon GDE; counter electrode: Pt mesh; electrode potentials: (●) -0.5, (□) -0.7, (△) -1.0, (◆) -1.3 V *vs.* Ag/AgCl. The solution contained 100 mg dm^{-3} of MB in 50 × 10^{-3} mol dm^{-3} of Na_2SO_4, 1 × 10^{-3} mol dm^{-3} of Fe^{+2} at temperature of 25 ºC and initial pH of 3 and oxygen flow rate of 0.15 cm^3 min^{-1}.

The degradation of the dye is significantly influenced by the applied potential. Thus, after 120 min of electrolysis at -0.5 V *vs.* Ag/AgCl, 68% of the colour was removed whereas, at -0.7 V *vs.* Ag/AgCl, as much as 97% was removed. No influence of the applied potential on the decolouration was observed at electrode potentials of -0.7, -1.0 and -1.3 V *vs.* Ag/AgCl. At these potentials, the MB decolourisation decreased below 99% of its original value after 240 min. The influence of the applied potential on the MB degradation is directly related to the concentration of electrogenerated hydrogen peroxide in solution which in the presence of Fe^{2+}, promotes the Fenton reaction [19, 46-48], via the powerful hydroxyl radical (•OH) oxidant according to reaction (1).

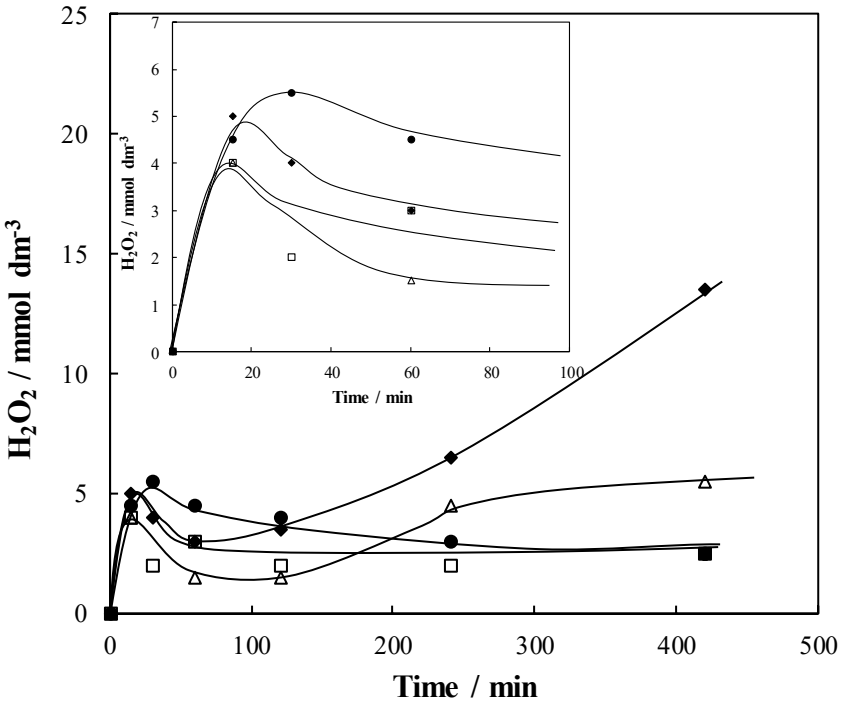

Fig. 3 Concentration of electrogenerated H_2O_2 as a function of time during the electrolysis of synthetic wastewater polluted with MB. Working electrode: carbon GDE; counter electrode: Pt mesh; electrode potentials: (●) -0.5, (□) -0.7, (△) -1.0, (◆) -1.3 V *vs.* Ag/AgCl. The solution contained 100 mg dm^{-3} of MB in 50×10^{-3} mol dm^{-3} of Na_2SO_4, 1×10^{-3} mol dm^{-3} of Fe^{2+} at 25 ºC and initial pH of 3 and an oxygen flow of 0.15 cm^3 min^{-1}. The inset shows the development of H_2O_2 concentration during the first 100 minutes of electrolysis.

The electrogeneration of hydrogen peroxide with the GDE working electrode at -0.5 V, -0.7 V, -1.0 V and -1.3 V *vs*. Ag/AgCl is shown in Fig. 3. Since the electrolysis was carried out in the presence of MB, it is important to highlight that this concentration corresponds to the hydrogen peroxide which did not react in solution and not the total electrogenerated hydrogen peroxide.

Hydrogen peroxide concentration increased to between 4.0 and 6.0 × 10^{-3} mol dm^{-3} within the first 30 min of electrolysis, and gradually decreased over time to a range between 2.0 and 4.0 × 10^{-3} mol dm^{-3} until 120 min. After this time, the concentration of hydrogen peroxide reached a steady-state content in solution, except for the electrode potential of -1.3 V *vs.* Ag/AgCl, which increased steadily up to 13 × 10^{-3} mol dm^{-3} at 420 minutes. The figure shows that the higher the electrode potential, the higher hydrogen peroxide concentration. The steady-state of hydrogen peroxide concentration in solution is a common behaviour widely reported in literature for electrolytic cells [19, 49, 50], as a consequence of the equilibrium between the electrogeneration rate of hydrogen peroxide at the cathode [reaction (3)] and its oxidation reaction rate at the anode to produce O_2 gas [reactions (5, 6)]. In addition, the anodic oxidation of water would provide dissolved oxygen through the following reactions:

$$H_2O_2 \rightarrow HO_2^{\bullet} + H^+ + e^- \quad (5)$$

$$HO_2^{\bullet} \rightarrow O_{2(g)} + H^+ + e^- \quad (6)$$

In this context, the presence of electrogenerated hydrogen peroxide according to reaction (3) in solution may partially help the degradation of organic dyes as the radical is more powerful oxidant [49, 51-53]. The hydrogen peroxide monitored in Figure 3 corresponds

to the hydrogen peroxide concentration which did not react with Fe^{2+} ions to produce the powerful hydroxyl radical oxidant following reaction (1). Hydroxyl radicals promote the mineralisation of a wide variety of organic pollutants such as alcohols, carboxylic acids, pharmaceuticals, pesticides, or dyes in aqueous solutions [3, 4, 54-57]. In Fig. 3, the concentration of hydrogen peroxide in solution at 240 min was 3.0, 2.0, 4.5 and 6.5 mM which corresponds to a MB decolourisation of 92, 100, 99 and 99% for -0.5 V, -0.7 V, -1.0 V and -1.3 V *vs*. Ag/AgCl, respectively. The highest hydrogen peroxide concentration detected in solution at 30 min for -0.5 V *vs.* Ag/AgCl resulted in the slowest dye decolourisation (16.5% dye degradation at 30 min) in Fig. 2. This suggests that the Fe^{3+} ion from Fenton's reaction is more slowly reduced to Fe^{2+} at the cathode surface during the electrolysis at -0.5 V *vs.* Ag/AgCl than at more negative electrode potentials.

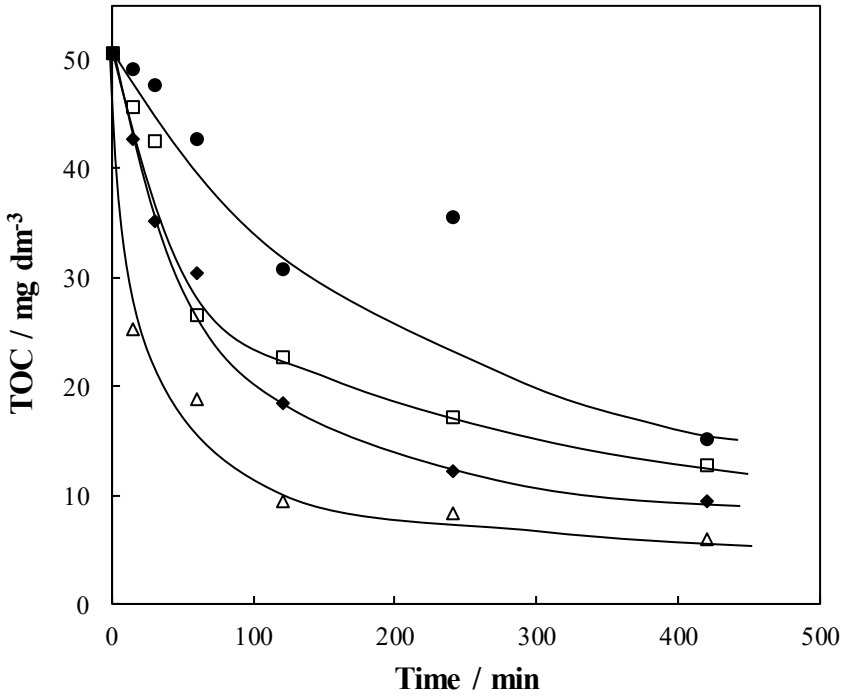

Fig. 4 Influence of applied potential on TOC decay during the electrolysis of synthetic wastewater polluted with MB. Working electrode: carbon GDE; counter electrode: Pt mesh; electrode potential: (●) -0.5, (□) -0.7, (△) -1.0, (◆) -1.3 V *vs.* Ag/AgCl. The solution contained 100 mg dm^{-3} of MB in 50×10^{-3} mol dm^{-3} of Na_2SO_4, 1×10^{-3} mol dm^{-3} of Fe^{+2} at temperature of 25 ºC and initial pH of 3 and oxygen flow rate of 0.15 cm^3 min^{-1}.

It is important to note that the dye should not only be degraded but also mineralised in order to minimise its hazardousness and that of its possible organic intermediates, before its final disposal into the aquatic environment. For that reason, the influence of the applied potential on the total organic carbon (TOC) decay during the electrolysis of synthetic wastewater contained 100 mg dm^{-3} MB was studied in Fig. 4.

The mineralisation of MB is significantly influenced by the applied electrode potential and likewise, it is observed to remain final mineralization percentages of 71, 75, 88 and 81% at -0.5, -0.7, -1.0 and -1.3 V *vs.* Ag/AgCl, respectively. The mineralisation of MB increased with the applied potential between -0.5 and -1.0 V *vs.* Ag/AgCl, although this behaviour was not observed at the electrode potential of -1.3 V *vs.* Ag/AgCl. The enhancement of TOC abatement with the increase of applied potential may be explained by the concomitant acceleration of all electrode reactions, giving rise to a greater quantity of the hydroxyl radicals from Fenton's reaction. However, at electrode potentials more negative than -1.0 V *vs.* Ag/AgCl the competitive reduction of H^+ to H_2 gas and/or the further two-electron reduction of H_2O_2 to OH^- predominates, thereby diminishing the rate of the oxygen reduction reaction to produce hydrogen peroxide and thus, it limits its ability to develop the Fenton's reaction [47, 49]. The highest TOC decay was developed at -1.0 V *vs.* Ag/AgCl and therefore, this potential was selected to study the influence of oxygen flow and counter electrode material on the degradation of MB.

Regarding the influence of oxygen flow rate, Fig. 5 shows the MB degradation during the electrolysis of synthetic wastewater polluted with 100 mg dm^{-3} MB at oxygen flow rates in the range of 0.15 – 0.45 cm^3 min^{-1}. The oxygen flows through the porous cathode which

supplies a much larger quantity of oxygen gas to the electrolyte-cathode surface promoting much higher concentrations of electrogenerated H_2O_2 [49]. At this point, the concentration of accumulated H_2O_2 was 0.16, 0.20 and 0.22 × 10^{-3} mol dm^{-3} during the electrolysis with oxygen flow rates of 0.15, 0.30 and 0.45 cm^3 min^{-1}, respectively.

The degradation rate of MB is not influenced by the oxygen flow rate under the experimental conditions studied, since MB degradation followed the same trend throughout the experimental time for each oxygen flow rate tested. Fig. 6 shows the influence of oxygen flow rate on the TOC decay during the electrolysis of synthetic wastewater polluted with MB. Here, the oxygen flow rate showed an influence on the mineralization of MB; the highest mineralization was achieved at the lowest oxygen flow rate. This may suggests that the cell configuration optimises the lowest oxygen flow rate through the porous cathode by promoting the efficient reduction of oxygen gas at the cathode surface to produce hydrogen peroxide and thus, avoiding the dispersion of oxygen gas bubbles through the GDE into the bulk solution which would result much less efficient process on the production of hydrogen peroxide [26-28].

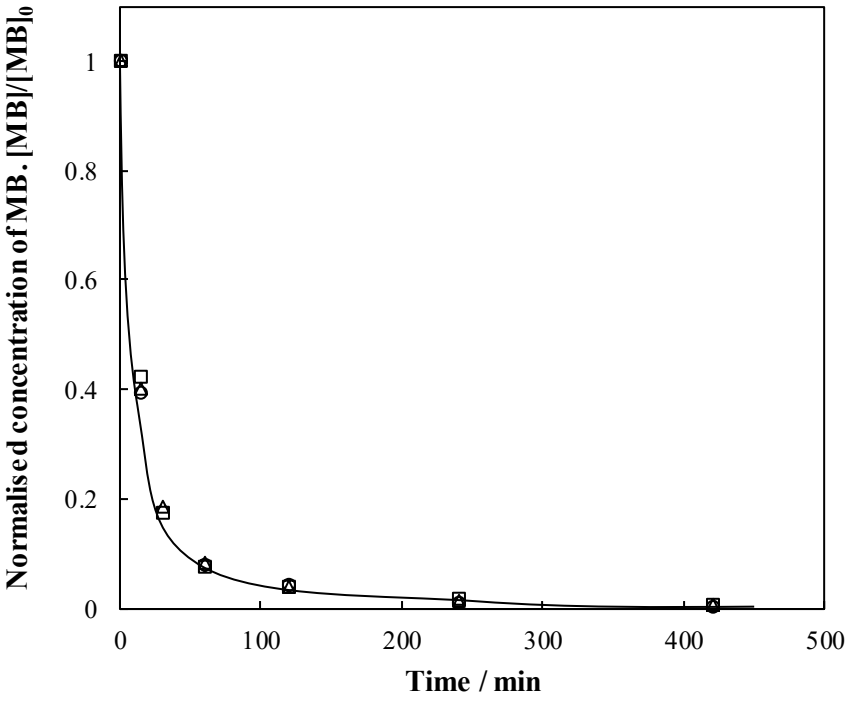

Fig. 5 Influence of oxygen flow on dye degradation during the electrolysis of synthetic wastewater polluted with MB. Working electrode: carbon GDE; counter electrode: Pt mesh; oxygen flow: (○) 0.15 cm^3 min^{-1}, (□) 0.30 cm^3 min^{-1}, (△) 0.45 cm^3 min^{-1}. The solution contained 100 mg dm^{-3} of MB in 50×10^{-3} mol dm^{-3} of Na_2SO_4, 1×10^{-3} mol dm^{-3} of Fe^{2+} at a temperature of 25 ºC and initial pH of 3 and electrode potential of -1.0 V *vs.* Ag/AgCl.

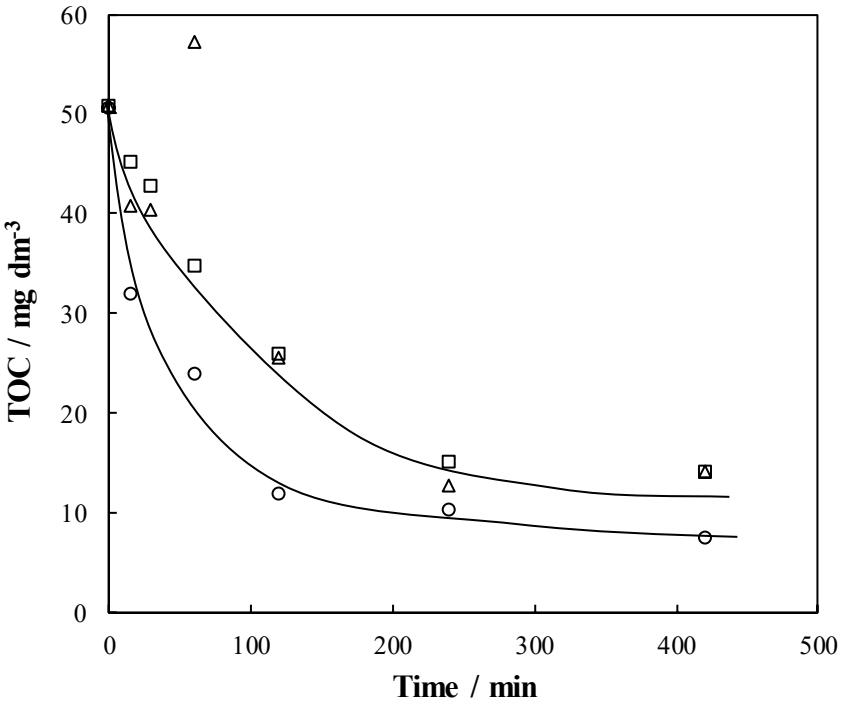

Fig. 6 Influence of oxygen flow on TOC decay during the electrolysis of synthetic wastewater polluted with MB. Working electrode: carbon GDE; counter electrode: Pt mesh; oxygen flow: (○) 0.15 cm^3 min^{-1}, (□) 0.30 cm^3 min^{-1}, (△) 0.45 cm^3 min^{-1}. The solution contained 100 mg dm^{-3} of MB in 50 × 10^{-3} mol dm^{-3} of Na_2SO_4, 1 × 10^{-3} mol dm^{-3} of Fe^{+2} at a temperature of 25 ºC, initial pH of 3 and an electrode potential of -1.0 V *vs.* Ag/AgCl.

Regarding the influence of the counter electrode material, Fig. 7 shows the TOC decay as function of the experimental time during the electrolysis of synthetic wastewater containing 100 mg dm^{-3} of MB. The counter electrode materials studied were Pt mesh (1 × 1 cm), Ni mesh (1 × 1 cm) and 100 ppi reticulated vitreous carbon (RVC) (1 × 1 × 0.15 cm).

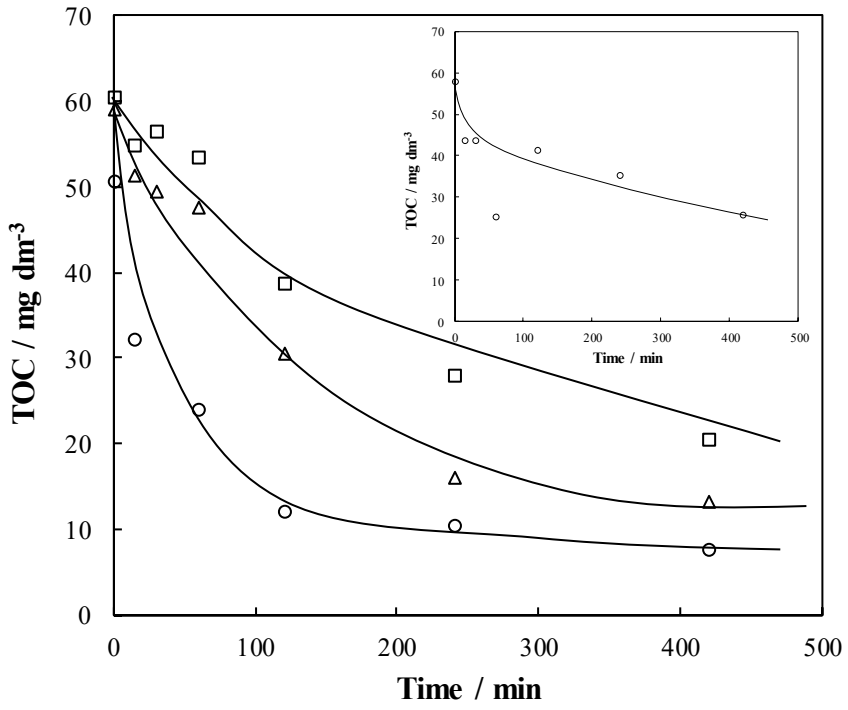

Fig. 7 Influence of counter electrode materials on the TOC decay during the electro-Fenton of synthetic wastewater containing MB at an electrode potential of -1.0 V *vs.* Ag/AgCl. Working electrode: carbon GDE; counter electrode: (○) Pt mesh, (□) Ni mesh, (△) RVC. The solution contained 100 mg dm^{-3} of MB in 50 × 10^{-3} mol dm^{-3} of Na_2SO_4, 1 × 10^{-3} mol dm^{-3} of Fe^{+2} at temperature of 25 ºC and initial pH of 3 and oxygen flow of 0.15 cm^3 min^{-1}. The inset shows the TOC decay during the anodic oxidation in the absence of Fe^{+2} ions under the same experimental conditions.

Although the MB is not completely mineralised under the experimental conditions studied, the TOC decay is significantly influenced by the counter electrode material. The TOC removal percentage is 66, 78 and 85% for RVC, Ni mesh and Pt mesh respectively, during the electro-Fenton process. The higher MB mineralisation was achieved with a Pt mesh counter electrode. This suggests that the MB is also oxidised at the Pt anode more rapidly than at Ni or RVC anodes. MB is probably strongly adsorbed on the Pt surface enhancing its reaction with Pt(•OH). In this way, the contribution of the anodic oxidation of MB (with a Pt anode and without adding Fe^{2+} catalyst) on the overall process is shown in the inset of Fig. 7. 78% TOC removal is achieved during the electro-Fenton process

whereas TOC removal percentage is mainly 56% for the anodic oxidation. This fact indicates that MB oxidation by Pt(•OH) is less efficient than the oxidation by homogeneous •OH. According to the literature, a Pt anode has been widely used to mineralise other organic compounds in wastewaters by electro-Fenton process such as 93.77% of rhodamine B [58], 92.2% of sulfamethazine [31], 87% of metoprolol tartrate [59], 49% of sulphanilamide [60] or 50% of aniline [61]. Nevertheless, Pt alone as an anode is reported to be unable to attain the complete mineralisation of refractory organic intermediates such as short carboxylic acids which remain in the final treated solutions [19, 62-65]. It was assumed that the formation of active chlorine and chlorine species did not contribute to dye degradation. High chlorine concentrations (100 – 3500 mg dm^{-3}) are normally required to significantly influence the degradation [20, 66]. Under the current experimental conditions, the concentration of chlorine is below 1.5 mg dm^{-3}.

In addition, the kinetic constants were calculated for the removal of MB (Fig. 8a) and TOC (Fig. 8b) as function of electrode potential. The exponential decay of TOC previously observed in Fig. 4, was well fitted to a pseudo-first order kinetic model by plotting ln (TOC_0/TOC) *vs*. experimental time and thus, yielding each kinetic constant for the electrode potential applied. The mineralisation process of a solution contained 100 mg dm^{-3} of MB in 50 × 10^{-3} mol dm^{-3} of Na_2SO_4, 1 × 10^{-3} mol dm^{-3} of Fe^{2+} at 25 ºC and an initial pH of 3 and oxygen flow rate of 0.15 cm^3 min^{-1} using a GDE working electrode and Pt mesh as counter electrode, was mass transport controlled [67, 68].

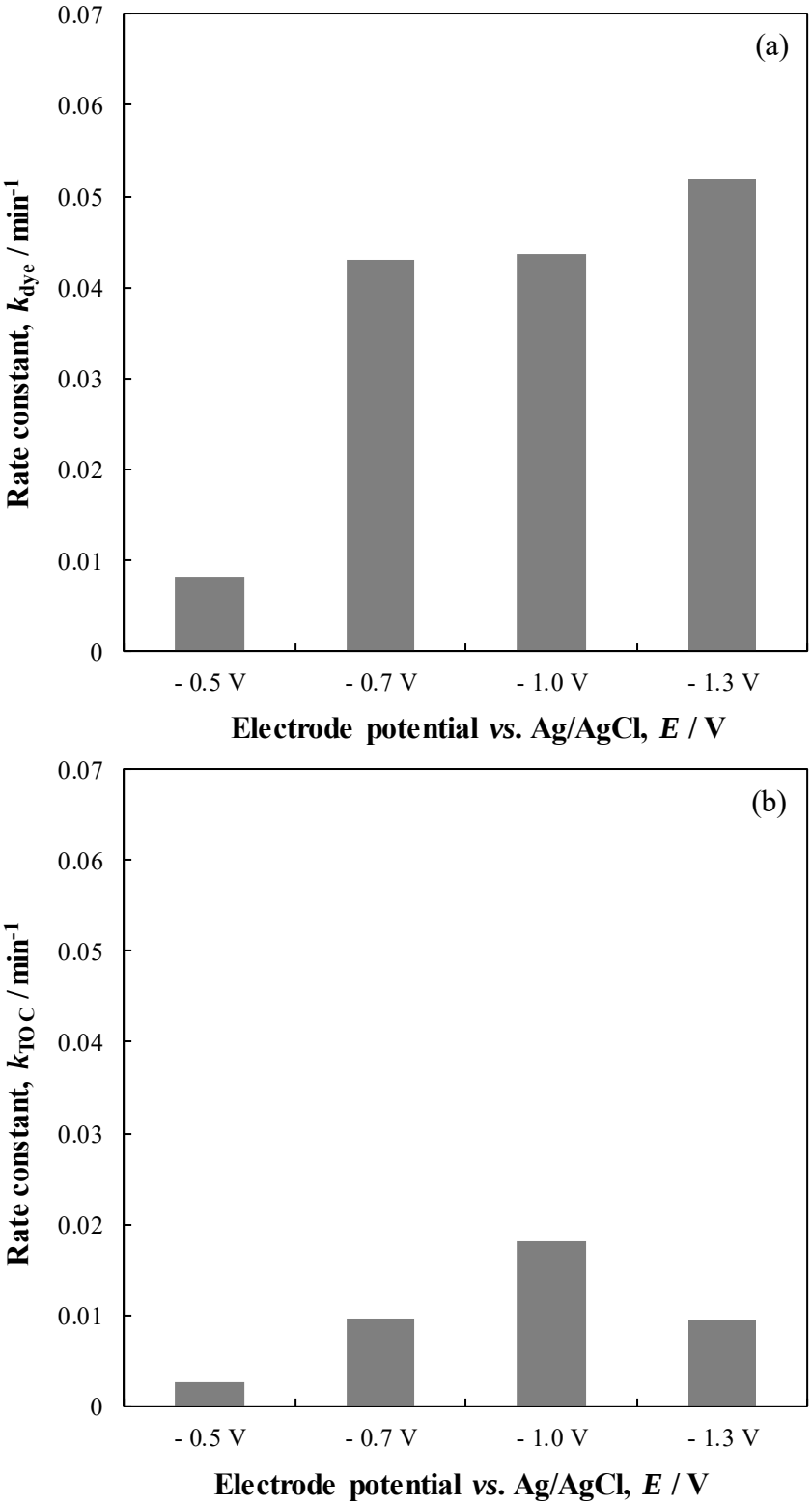

Fig. 8 Apparent first order rate kinetic constants calculated for the removal of dye (a) and TOC (b) as function of electrode potential (V *vs.* Ag/AgCl) by using GDE as working electrode and Pt mesh as counter electrode. The solution contained 100 mg dm^{-3} of MB in 50 × 10^{-3} mol dm^{-3} of Na_2SO_4, 1 × 10^{-3} mol dm^{-3} of Fe^{+2} at temperature of 25 ºC, an initial pH of 3 and an oxygen flow rate of 0.15 cm^3 min^{-1}.

Kinetic constants for MB decolourisation increase as function of the applied electrode potential, within a range from 0.0081 to 0.0520 min^{-1}. These kinetic constants are lower than some values reported in the literature, for example kinetic constants values of 0.097 min^{-1} and 0.177 min^{-1} for the degradation of 50 mg dm^{-3} and 5 mg dm^{-3} MB were reported in a non-thermal microwave plasma jet at atmospheric pressure [69]. Although these kinetic constants are higher, the amount of MB was lower than in the present investigation. Here, the normalised space velocity (s_n) was calculated for a 90% of MB decolourisation to characterise the performance of the electrochemical cell according to equation (7) [70]. Furthermore, the reaction rate is completely mass transport controlled in many cases and the reactant degradation is limited by its rate of convective diffusion to the electrode. Then, the mass transport coefficient (k_m) was also calculated by following equation (8) and data are shown in Table 1.

$$s_n = \frac{I \cdot \emptyset}{V_R \cdot z \cdot F} \tag{7}$$

$$\ln\left(\frac{c_t}{c_0}\right) = -\frac{k_m \cdot A}{V_R} t \tag{8}$$

where I is the current (A), $\emptyset$ is the overall current efficiency, V_R is the reactor volume (m^3), z is the number of electrons transferred, F is the Faraday constant (96485 C mol^{-1}), c_t in the concentration at time t (mol m^{-3}), c_0 is the concentration at time zero (mol m^{-3}) and A is the active electrode area (m^2).

The s_n values shown in Table 1 are one order of magnitude lower in comparison with 1.76 $m^3\ m^{-3}\ h^{-1}$ obtained for the 88% of MB decolouration by using an initial MB concentration of 100 mg dm^{-3} at 42.55 mA cm^{-2} in a cell with graphite as anode and stainless steel as cathode [71]. This may be due to the large volume of the electrolyte (300 cm^3) in comparison to the small electrode area (1 cm^2) employed. Otherwise, k_m values shown in

Table 1 are one order of magnitude higher than those values found in literature, 0.001 m h^{-1} [72] and 0.015 m h^{-1} [73], for the removal of organic dyes by electrochemical oxidation processes.

Table 1. Normalised space velocity and mass transport coefficient values as function of electrode potential during electro-Fenton process for MB removal.

***E* (V *vs.* Ag/AgCl)**	**s_n (m^3 m^{-3} h^{-1})**	**k_m (m s^{-1})**
- 0.5	0.08	0.215
- 0.7	0.28	0.815
- 1.0	0.30	0.753
- 1.3	0.32	1.253

Likewise, kinetic constants for MB mineralisation are observed to increase as function of applied electrode potential, although a maximum apparent first order rate kinetic constant value of 0.0182 min^{-1} is calculated for -1.0 V *vs.* Ag/AgCl. Apparent batch decay rate constants for MB decolouration are observed to be three times higher than those calculated for MB mineralisation. TMB is more rapidly degraded to colourless intermediate products which are mineralised much more slowly under the experimental conditions.

Finally, Fig. 9 shows the current efficiency calculated for the dye degradation during the electrolysis of synthetic wastewater containing 100 mg dm^{-3} of MB by using different counter electrode materials: RVC, Ni mesh and Pt mesh. The current was also monitored and varied from 10 to 15 mA, regardless of the counter electrode material being tested. The current efficiency was calculated using Eq. (9):

$$\% \text{ Current efficiency} = \frac{F \cdot \sum[\Delta n \cdot z]}{I \cdot \Delta t} \cdot 100 \quad (9)$$

where F is the Faraday constant (96485 C mol^{-1}), Δn is the amount of MB decolourised over the time interval Δt, z is the number of electrons exchanged in reaction (10) and I is the current applied. It is noteworthy that a high electron stoichiometry (77 e^-) is needed to achieve complete MB degradation by direct electrolysis as shown in reaction (10), making an efficient, mediated indirect route important to realise a feasible process.

$$C_{16}H_{18}ClN_3S + 34H_2O \rightarrow 16CO_2 + ½Cl_2 + 3NH_4^+ + SO_2 + 74H^+ + 77e^- \quad (10)$$

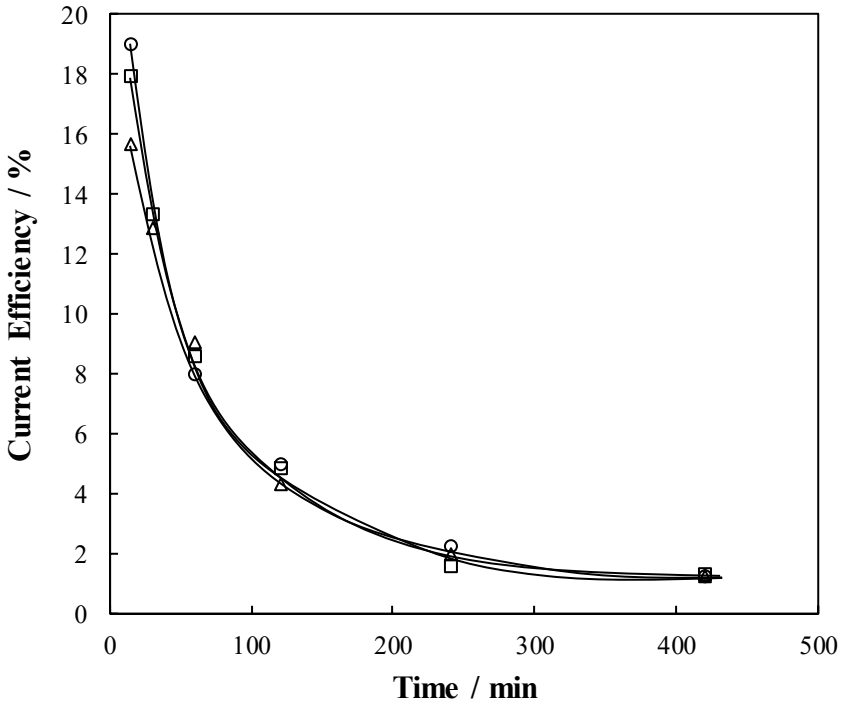

Fig. 9. Variation of overall current efficiency with time during the electrolysis of synthetic wastewater polluted with MB. Working electrode: GDE; counter electrode: (○) Pt mesh, (□) Ni mesh, (△) RVC. The solution contained 100 mg dm^{-3} of MB in 50 × 10^{-3} mol dm^{-3} of Na_2SO_4, 1 × 10^{-3} mol dm^{-3} of Fe^{2+} at temperature of 25 ºC and initial pH of 3, an oxygen flow rate of 0.15 cm^3 min^{-1} and an electrode potential of -1.0 V *vs.* Ag/AgCl.

The current efficiency is low and decreased exponentially with time. This is a typical trend in an electrochemical mass transfer controlled processes as a result of the decrease in the amount of reactant available to be oxidized [74, 75]. Likewise, initial current

efficiency depends on the counter electrode material and is only slightly higher in the order Pt mesh > Ni mesh > RVC. In particular, initial current efficiencies were of 16, 18 and 20 % for RVC, Ni mesh and Pt mesh counter electrodes, respectively. In literature, there are few papers reporting the influence of anode materials in the electro-Fenton process and these reports are mainly focused on the effect of most common anode materials used in electro-oxidation: Pt and boron doped diamond (BDD) [31, 76, 77]. In this way, the electro-Fenton process with Pt anode is reported a mineralisation current efficiency (MCE) of 20% for 90% of TOC removal from initial 0.1 mol dm^{-3} rhodamine B [58], less than 30% of MCE for 50% of TOC removal from an initial 92 mg dm^{-3} 2,4-D [78] or less than 5% of MCE for 95% of TOC removal from initial 0.15×10^{-3} mol dm^{-3} ciprofloxacin hydrochloride [35].

4. Conclusions

From this work, the following conclusions can be drawn:

- An electro-Fenton process using gas diffusion electrodes attained the complete decolourisation of methylene blue at electrode potentials more negative than -0.7 V *vs.* Ag/AgCl.

- The applied electrode potential had a significant influence on the mineralisation of methylene blue, a maximum mineralisation of 88% being found at -1.0 V *vs.* Ag/AgCl.

- The oxygen flow rate to the gas diffusion electrode during hydrogen peroxide production, was observed not to have an influence on methylene blue degradation under the experimental conditions studied.

- The counter electrode material led to obtain a mineralisation of 85%, 78% and 66% when Pt mesh, Ni mesh and RVC were used, respectively.

- The methylene blue decay followed a first order reaction and kinetic constants for methylene blue degradation were observed to be three times higher than those calculated for mineralisation of the dye.

- The normalised space velocity (*NSV*) s_n, varied between 0.08 m^3 m^{-3} h^{-1} and 0.32 m^3 m^{-3} h^{-1} whereas the mass transfer coefficient k_m, varied between 0.215 m s^{-1} to 1.253 m s^{-1} both as a function of the applied electrode potential between - 0.5 V to - 1.3 V *vs*. Ag/AgCl. The two values are within the order of magnitude reported for other electrochemical process.

- Among the highlights of this paper is report of the normalised space velocity as a figure of merit which is fundamental for reactor modelling and scale up operations. Despite its importance it is rarely reported in papers reporting the oxidation of organic materials in waste water.

Acknowledgements

The authors acknowledge funding support from European Union and Spanish Government through MINECO Project CTM2016-76197-R (AEI/FEDER, UE). Engracia Lacasa acknowledges the financial support from Vicerrectorado de Profesorado, University of Castilla-La Mancha, Spain to visit the University of Southampton.

References

[1] R. López Cisneros, A. Gutarra Espinoza, M.I. Litter, Photodegradation of an azo dye of the textile industry, Chemosphere, 48 (2002) 393-399.

[2] A.J. Méndez-Martínez, M.M. Dávila-Jiménez, O. Ornelas-Dávila, M.P. Elizalde-González, U. Arroyo-Abad, I. Sirés, E. Brillas, Electrochemical reduction and oxidation pathways for Reactive Black 5 dye using nickel electrodes in divided and undivided cells, Electrochimica Acta, 59 (2012) 140-149.

[3] K. Shoueir, H. El-Sheshtawy, M. Misbah, H. El-Hosainy, I. El-Mehasseb, M. El-Kemary, Fenton-like nanocatalyst for photodegradation of methylene blue under visible light activated by hybrid green DNSA@Chitosan@$MnFe_2O_4$, Carbohydrate Polymers, 197 (2018) 17-28.

[4] Z.F. Cao, X. Wen, P. Chen, F. Yang, X.L. Ou, S. Wang, H. Zhong, Synthesis of a novel heterogeneous fenton catalyst and promote the degradation of methylene blue by fast regeneration of Fe^{2+}, Colloids and Surfaces A: Physicochemical and Engineering Aspects, 549 (2018) 94-104.

[5] M. Rafatullah, O. Sulaiman, R. Hashim, A. Ahmad, Adsorption of methylene blue on low-cost adsorbents: A review, Journal of Hazardous Materials, 177 (2010) 70-80.

[6] H. Dai, Y. Huang, H. Huang, Eco-friendly polyvinyl alcohol/carboxymethyl cellulose hydrogels reinforced with graphene oxide and bentonite for enhanced adsorption of methylene blue, Carbohydrate Polymers, 185 (2018) 1-11.

[7] M. Cheng, G. Zeng, D. Huang, C. Lai, Y. Liu, C. Zhang, R. Wang, L. Qin, W. Xue, B. Song, S. Ye, H. Yi, High adsorption of methylene blue by salicylic acid–methanol modified steel converter slag and evaluation of its mechanism, Journal of Colloid and Interface Science, 515 (2018) 232-239.

[8] J. Xu, D. Xu, B. Zhu, B. Cheng, C. Jiang, Adsorptive removal of an anionic dye Congo Red by flower-like hierarchical magnesium oxide (MgO)-graphene oxide composite microspheres, Applied Surface Science, 435 (2018) 1136-1142.

[9] Q. Yang, S. Ren, Q. Zhao, R. Lu, C. Hang, Z. Chen, H. Zheng, Selective separation of methyl orange from water using magnetic ZIF-67 composites, Chemical Engineering Journal, 333 (2018) 49-57.

[10] S. De Gisi, G. Lofrano, M. Grassi, M. Notarnicola, Characteristics and adsorption capacities of low-cost sorbents for wastewater treatment: A review, Sustainable Materials and Technologies, 9 (2016) 10-40.

[11] M.T. Yagub, T.K. Sen, S. Afroze, H.M. Ang, Dye and its removal from aqueous solution by adsorption: A review, Advances in Colloid and Interface Science, 209 (2014) 172-184.

[12] J. Wang, Z. Bai, Fe-based catalysts for heterogeneous catalytic ozonation of emerging contaminants in water and wastewater, Chemical Engineering Journal, 312 (2017) 79-98.

[13] S. Larouk, R. Ouargli, D. Shahidi, L. Olhund, T.C. Shiao, N. Chergui, T. Sehili, R. Roy, A. Azzouz, Catalytic ozonation of Orange-G through highly interactive contributions of hematite and SBA-16 – To better understand azo-dye oxidation in nature, Chemosphere, 168 (2017) 1648-1657.

[14] M. Solís, A. Solís, H.I. Pérez, N. Manjarrez, M. Flores, Microbial decolouration of azo dyes: A review, Process Biochemistry, 47 (2012) 1723-1748.

[15] H. Li, M. Li, L. Zhang, X. Zhang, Y. Ma, B. Yu, Q. Wei, S. Yin, Dipyridylbenzene as a charming sensitizer to significantly enhance the photocatalytic activity of titanium dioxide, Applied Catalysis B: Environmental, 232 (2018) 472-480.

[16] Y. Shen, Q. Xu, D. Gao, H. Shi, Degradation of an anthraquinone dye by ozone/Fenton: response surface approach and degradation pathway, Ozone: Science and Engineering, 39 (2017) 219-232.

[17] A.R. Ribeiro, O.C. Nunes, M.F.R. Pereira, A.M.T. Silva, An overview on the advanced oxidation processes applied for the treatment of water pollutants defined in the recently launched Directive 2013/39/EU, Environment International, 75 (2015) 33-51.

[18] V. Khandegar, A.K. Saroha, Electrocoagulation for the treatment of textile industry effluent - A review, Journal of Environmental Management, 128 (2013) 949-963.

[19] E. Brillas, C.A. Martínez-Huitle, Decontamination of wastewaters containing synthetic organic dyes by electrochemical methods. An updated review, Applied Catalysis B: Environmental, 166-167 (2015) 603-643.

[20] S. Cotillas, J. Llanos, P. Cañizares, D. Clematis, G. Cerisola, M.A. Rodrigo, M. Panizza, Removal of Procion Red MX-5B dye from wastewater by conductive-diamond electrochemical oxidation, Electrochimica Acta, 263 (2018) 1-7.

[21] S. Cotillas, D. Clematis, P. Cañizares, M.P. Carpanese, M.A. Rodrigo, M. Panizza, Degradation of dye Procion Red MX-5B by electrolytic and electro-irradiated technologies using diamond electrodes, Chemosphere, 199 (2018) 445-452.

[22] C. Zhang, Y. Jiang, Y. Li, Z. Hu, L. Zhou, M. Zhou, Three-dimensional electrochemical process for wastewater treatment: A general review, Chemical Engineering Journal, 228 (2013) 455-467.

[23] E.J. Ruiz, C. Arias, E. Brillas, A. Hernández-Ramírez, J.M. Peralta-Hernández, Mineralization of Acid Yellow 36azo dye by electro-Fenton and solar photoelectro-Fenton processes with a boron-doped diamond anode, Chemosphere, 82 (2011) 495-501.

[24] C.A. Martínez-Huitle, E. Brillas, Decontamination of wastewaters containing synthetic organic dyes by electrochemical methods: A general review, Applied Catalysis B: Environmental, 87 (2009) 105-145.

[25] A.J. Poole, Treatment of biorefractory organic compounds in wool scour effluent by hydroxyl radical oxidation, Water Research, 38 (2004) 3458-3464.

[26] E. Brillas, I. Sirés, M.A. Oturan, Electro-fenton process and related electrochemical technologies based on fenton's reaction chemistry, Chemical Reviews, 109 (2009) 6570-6631.

[27] A.R. Khataee, M. Safarpour, M. Zarei, S. Aber, Electrochemical generation of H_2O_2 using immobilized carbon nanotubes on graphite electrode fed with air: Investigation of operational parameters, Journal of Electroanalytical Chemistry, 659 (2011) 63-68.

[28] T. Harrington, D. Pletcher, Removal of low levels of organics from aqueous solutions using Fe(II) and hydrogen peroxide formed in situ at gas diffusion electrodes, Journal of the Electrochemical Society, 146 (1999) 2983-2989.

[29] A. Khataee, A. Khataee, M. Fathinia, B. Vahid, S.W. Joo, Kinetic modeling of photoassisted-electrochemical process for degradation of an azo dye using boron-doped diamond anode and cathode with carbon nanotubes, Journal of Industrial and Engineering Chemistry, 19 (2013) 1890-1894.

[30] A. Khataee, A. Akbarpour, B. Vahid, Photoassisted electrochemical degradation of an azo dye using Ti/RuO_2 anode and carbon nanotubes containing gas-diffusion cathode, Journal of the Taiwan Institute of Chemical Engineers, 45 (2014) 930-936.

[31] F. Sopaj, N. Oturan, J. Pinson, F. Podvorica, M.A. Oturan, Effect of the anode materials on the efficiency of the electro-Fenton process for the mineralization of the antibiotic sulfamethazine, Applied Catalysis B: Environmental, 199 (2016) 331-341.

[32] L.F. Castañeda, F.C. Walsh, J.L. Nava, C. Ponce de León, Graphite felt as a versatile electrode material: Properties, reaction environment, performance and applications, Electrochimica Acta, 258 (2017) 1115-1139.

[33] A. Wang, J. Qu, H. Liu, J. Ru, Mineralization of an azo dye Acid Red 14 by photoelectro-Fenton process using an activated carbon fiber cathode, Applied Catalysis B: Environmental, 84 (2008) 393-399.

[34] M.H.M.T. Assumpção, A. Moraes, R.F.B. De Souza, R.M. Reis, R.S. Rocha, I. Gaubeur, M.L. Calegaro, P. Hammer, M.R.V. Lanza, M.C. Santos, Degradation of dipyrone via advanced oxidation processes using a cerium nanostructured electrocatalyst material, Applied Catalysis A: General, 462-463 (2013) 256-261.

[35] M.S. Yahya, N. Oturan, K. El Kacemi, M. El Karbane, C.T. Aravindakumar, M.A. Oturan, Oxidative degradation study on antimicrobial agent ciprofloxacin by electro-fenton process: Kinetics and oxidation products, Chemosphere, 117 (2014) 447-454.

[36] S.O. Ganiyu, T.X. Huong Le, M. Bechelany, G. Esposito, E.D. Van Hullebusch, M.A. Oturan, M. Cretin, A hierarchical CoFe-layered double hydroxide modified carbon-felt cathode for heterogeneous electro-Fenton process, Journal of Materials Chemistry A, 5 (2017) 3655-3666.

[37] N. Borràs, R. Oliver, C. Arias, E. Brillas, Degradation of atrazine by electrochemical advanced oxidation processes using a boron-doped diamond anode, Journal of Physical Chemistry A, 114 (2010) 6613-6621.

[38] A. Thiam, I. Sirés, J.A. Garrido, R.M. Rodríguez, E. Brillas, Decolorization and mineralization of Allura Red AC aqueous solutions by electrochemical advanced oxidation processes, Journal of Hazardous Materials, 290 (2015) 34-42.

[39] J.M. Friedrich, C. Ponce-de-León, G.W. Reade, F.C. Walsh, Reticulated vitreous carbon as an electrode material, Journal of Electroanalytical Chemistry, 561 (2004) 203-217.

[40] F.C. Walsh, L.F. Arenas, C. Ponce de León, G.W. Reade, I. Whyte, B.G. Mellor, The continued development of reticulated vitreous carbon as a versatile electrode material: Structure, properties and applications, Electrochimica Acta, 215 (2016) 566-591.

[41] K. Cruz-González, O. Torres-Lopez, A.M. García-León, E. Brillas, A. Hernández-Ramírez, J.M. Peralta-Hernández, Optimization of electro-Fenton/BDD process for decolorization of a model azo dye wastewater by means of response surface methodology, Desalination, 286 (2012) 63-68.

[42] R.D. McKerracher, C. Alegre, V. Baglio, A.S. Aricò, C. Ponce de León, F. Mornaghini, M. Rodlert, F.C. Walsh, A nanostructured bifunctional Pd/C gas-diffusion electrode for metal-air batteries, Electrochimica Acta, 174 (2015) 508-515.

[43] R.D. McKerracher, H.A. Figueredo-Rodríguez, C. Ponce de León, C. Alegre, V. Baglio, A.S. Aricò, F.C. Walsh, A high-performance, bifunctional oxygen electrode catalysed with palladium and nickel-iron hexacyanoferrate, Electrochimica Acta, 206 (2016) 127-133.

[44] F.C. Walsh, C. Ponce de León, Progress in electrochemical flow reactors for laboratory and pilot scale processing, Electrochimica Acta, 280 (2018) 121-148.

[45] A.I. Vogel, Vogel's textbook of quantitative chemical analysis, in: J. Mendham, R.C. Denney, J.D. Barnes, M. Thomas (Eds.), Prentice Hall, Harlow, England ;, 2000.

[46] V. Poza-Nogueiras, E. Rosales, M. Pazos, M. Sanromán, Current advances and trends in electro-Fenton process using heterogeneous catalysts – A review, Chemosphere, 201 (2018) 399-416.

[47] I. Sirés, E. Brillas, M.A. Oturan, M.A. Rodrigo, M. Panizza, Electrochemical advanced oxidation processes: today and tomorrow. A review, Environmental Science and Pollution Research, 21 (2014) 8336-8367.

[48] O. Scialdone, A. Galia, C. Gattuso, S. Sabatino, B. Schiavo, Effect of air pressure on the electro-generation of H_2O_2 and the abatement of organic pollutants in water by electro-Fenton process, Electrochimica Acta, 182 (2015) 775-780.

[49] J.A. Bañuelos, O. García-Rodríguez, A. El-Ghenymy, F.J. Rodríguez-Valadez, L.A. Godínez, E. Brillas, Advanced oxidation treatment of malachite green dye using a low cost carbon-felt air-diffusion cathode, Journal of Environmental Chemical Engineering, 4 (2016) 2066-2075.

[50] A. El-Ghenymy, N. Oturan, M.A. Oturan, J.A. Garrido, P.L. Cabot, F. Centellas, R.M. Rodríguez, E. Brillas, Comparative electro-Fenton and UVA photoelectro-Fenton degradation of the antibiotic sulfanilamide using a stirred BDD/air-diffusion tank reactor, Chemical Engineering Journal, 234 (2013) 115-123.

[51] V.M. Vasconcelos, C. Ponce-de-León, J.L. Nava, M.R.V. Lanza, Electrochemical degradation of RB-5 dye by anodic oxidation, electro-Fenton and by combining anodic oxidation–electro-Fenton in a filter-press flow cell, Journal of Electroanalytical Chemistry, 765 (2016) 179-187.

[52] C. Ridruejo, F. Centellas, P.L. Cabot, I. Sirés, E. Brillas, Electrochemical Fenton-based treatment of tetracaine in synthetic and urban wastewater using active and non-active anodes, Water Research, 128 (2018) 71-81.

[53] S. Garcia-Segura, F. Centellas, C. Arias, J.A. Garrido, R.M. Rodríguez, P.L. Cabot, E. Brillas, Comparative decolorization of monoazo, diazo and triazo dyes by electro-Fenton process, Electrochimica Acta, 58 (2011) 303-311.

[54] A.A. Özcan, A. Özcan, Investigation of applicability of Electro-Fenton method for the mineralization of naphthol blue black in water, Chemosphere, 202 (2018) 618-625.

[55] X. Liu, C. Sun, L. Chen, H. Yang, Z. Ming, Y. Bai, S. Feng, S.T. Yang, Decoloration of methylene blue by heterogeneous Fenton-like oxidation on $Fe_3O_4/SiO_2/C$ nanospheres in neutral environment, Materials Chemistry and Physics, 213 (2018) 231-238.

[56] S.O. Ganiyu, M. Zhou, C.A. Martínez-Huitle, Heterogeneous electro-Fenton and photoelectro-Fenton processes: A critical review of fundamental principles and application for water/wastewater treatment, Applied Catalysis B: Environmental, 235 (2018) 103-129.

[57] M.A. Rodrigo, N. Oturan, M.A. Oturan, Electrochemically assisted remediation of pesticides in soils and water: a review, Chemical reviews, 114 (2014) 8720-8745.

[58] J. Tian, A.M. Olajuyin, T. Mu, M. Yang, J. Xing, Efficient degradation of rhodamine B using modified graphite felt gas diffusion electrode by electro-Fenton process, Environmental Science and Pollution Research, 23 (2016) 11574-11583.

[59] E. Isarain-Chávez, J.A. Garrido, R.M. Rodríguez, F. Centellas, C. Arias, P.L. Cabot, E. Brillas, Mineralization of Metoprolol by electro-Fenton and photoelectro-Fenton processes, The Journal of Physical Chemistry A, 115 (2011) 1234-1242.

[60] A. El-Ghenymy, P.L. Cabot, F. Centellas, J.A. Garrido, R.M. Rodríguez, C. Arias, E. Brillas, Mineralization of sulfanilamide by electro-Fenton and solar photoelectro-Fenton in a pre-pilot plant with a Pt/air-diffusion cell, Chemosphere, 91 (2013) 1324-1331.

[61] J. Casado, J. Fornaguera, M.I. Galán, Mineralization of aromatics in water by sunlight-assisted electro-Fenton technology in a pilot reactor, Environmental Science & Technology, 39 (2005) 1843-1847.

[62] I. Sirés, P.L. Cabot, F. Centellas, J.A. Garrido, R.M. Rodríguez, C. Arias, E. Brillas, Electrochemical degradation of clofibric acid in water by anodic oxidation: Comparative study with platinum and boron-doped diamond electrodes, Electrochimica Acta, 52 (2006) 75-85.

[63] M. Hamza, R. Abdelhedi, E. Brillas, I. Sirés, Comparative electrochemical degradation of the triphenylmethane dye Methyl Violet with boron-doped diamond and Pt anodes, Journal of Electroanalytical Chemistry, 627 (2009) 41-50.

[64] E.B. Cavalcanti, S. García-Segura, F. Centellas, E. Brillas, Electrochemical incineration of omeprazole in neutral aqueous medium using a platinum or boron-doped diamond anode: degradation kinetics and oxidation products, Water Research, 47 (2013) 1803-1815.

[65] F.C. Moreira, S. Garcia-Segura, V.J.P. Vilar, R.A.R. Boaventura, E. Brillas, Decolorization and mineralization of Sunset Yellow FCF azo dye by anodic oxidation, electro-Fenton, UVA photoelectro-Fenton and solar photoelectro-Fenton processes, Applied Catalysis B: Environmental, 142-143 (2013) 877-890.

[66] G.A. Cerrón-Calle, A.J. Aranda-Aguirre, C. Luyo, S. Garcia-Segura, H. Alarcón, Photoelectrocatalytic decolorization of azo dyes with nano-composite oxide layers of ZnO nanorods decorated with Ag nanoparticles, Chemosphere, 219 (2019) 296-304.

[67] L.V. Jian-Xiao, C. Ying, X. Guo-Hong, Z. Ling-Yun, W. Su-Fen, Decoloration of methylene blue simulated wastewater using a UV-H_2O_2 combined system, Journal of Water Reuse and Desalination, 1 (2011) 45-51.

[68] R.R. Aquino, M.S. Tolentino, B.M.Z. Crisogono, S.K.V. Salvacion, Adsorption of methylene blue (MB) dye in wastewater by electrospun polysulfone (PSF)/organo-montmorillonite (O-MMT) nanostructured membrane, Materials Science Forum, 2018, pp. 120-124.

[69] M.C. García, M. Mora, D. Esquivel, J.E. Foster, A. Rodero, C. Jiménez-Sanchidrián, F.J. Romero-Salguero, Microwave atmospheric pressure plasma jets for wastewater treatment: Degradation of methylene blue as a model dye, Chemosphere, 180 (2017) 239-246.

[70] F.C. Walsh, Determination of the normalised space velocity for continuous stirred tank electrochemical reactors, Electrochimica Acta, 38 (1993) 465-468.

[71] M.H. Abdel-Aziz, M. Bassyouni, M.S. Zoromba, A.A. Alshehri, Removal of Dyes from Waste Solutions by Anodic Oxidation on an Array of Horizontal Graphite Rods Anodes, Industrial & Engineering Chemistry Research, (2018).

[72] M.R. Cruz-Díaz, E.P. Rivero, F.A. Rodríguez, R. Domínguez-Bautista, Experimental study and mathematical modeling of the electrochemical degradation of dyeing wastewaters in presence of chloride ion with dimensional stable anodes (DSA) of expanded meshes in a FM01-LC reactor, Electrochimica Acta, 260 (2018) 726-737.

[73] F. Rivera Fernando, A. Rodríguez Francisca, P. Rivero Eligio, R. Cruz-Díaz Martín, Parametric mathematical modelling of Cristal Violet dye electrochemical oxidation using a flow electrochemical reactor with BDD and DSA anodes in sulfate media, International Journal of Chemical Reactor Engineering, 2018.

[74] J. Robles-Molina, M.J. Martín de Vidales, J.F. García-Reyes, P. Cañizares, C. Sáez, M.A. Rodrigo, A. Molina-Díaz, Conductive-diamond electrochemical oxidation of chlorpyrifos in wastewater and identification of its main degradation products by LC-TOFMS, Chemosphere, 89 (2012) 1169-1176.

[75] M.J. Martín de Vidales, J. Robles-Molina, J.C. Domínguez-Romero, P. Cañizares, C. Sáez, A. Molina-Díaz, M.A. Rodrigo, Removal of sulfamethoxazole from waters and wastewaters by conductive-diamond electrochemical oxidation, Journal of Chemical Technology and Biotechnology, 87 (2012) 1441-1449.

[76] A. Özcan, Y. Şahin, A.S. Koparal, M.A. Oturan, A comparative study on the efficiency of electro-Fenton process in the removal of propham from water, Applied Catalysis B: Environmental, 89 (2009) 620-626.

[77] N. Oturan, E. Brillas, M.A. Oturan, Unprecedented total mineralization of atrazine and cyanuric acid by anodic oxidation and electro-Fenton with a boron-doped diamond anode, Environmental Chemistry Letters, 10 (2012) 165-170.

[78] O. García, E. Isarain-Chávez, A. El-Ghenymy, E. Brillas, J.M. Peralta-Hernández, Degradation of 2,4-D herbicide in a recirculation flow plant with a Pt/air-diffusion and a BDD/BDD cell by electrochemical oxidation and electro-Fenton process, Journal of Electroanalytical Chemistry, 728 (2014) 1-9.